

Phase diagram of a 1 dimensional spin-orbital model

Chigak Itoi^{1,2}, Shaojin Qin^{1,3}, and Ian Affleck^{1,4,5}

¹ Department of physics and astronomy, University of British Columbia, Vancouver, BC, V6T1Z1, Canada

² Department of Physics, Nihon University, Kanda, Surugadai, Chiyoda, Tokyo, Japan

³ Institute of Theoretical Physics, CAS, Beijing 100080, P R China

⁴ Canadian Institute for Advanced Research, The University of British Columbia, Vancouver, B.C., V6T 1Z1, Canada

⁵ Institute for Theoretical Physics, University of California, Santa Barbara, CA93106-4030

(September 24, 2018)

We study a 1 dimensional spin-orbital model using both analytical and numerical methods. Renormalization group calculations are performed in the vicinity of a special integrable point in the phase diagram with $SU(4)$ symmetry. These indicate the existence of a gapless phase in an extended region of the phase diagram, missed in previous studies. This phase is $SU(4)$ invariant at low energies apart from the presence of different velocities for spin and orbital degrees of freedom. The phase transition into a gapped dimerized phase is in a generalized Kosterlitz-Thouless universality class. The phase diagram of this model is sketched using the density matrix renormalization group technique.

PACS: 75.10.Jm, 11.10.Hi, 11.25.Hf, 75.40Mg

I. INTRODUCTION

Spin-orbital models arise in many kinds of materials. They have been derived for C_{60} material¹, $LiNiO_2$ samples², and degenerate chains in $Na_2Ti_2Sb_2O$ compound³. In this paper we study a one dimensional $SU(2) \times SU(2)$ spin-orbital model with Hamiltonian:

$$H = \sum_i (x + \vec{S}_i \cdot \vec{S}_{i+1})(y + \vec{T}_i \cdot \vec{T}_{i+1}). \quad (1.1)$$

where S_i^a and T_i^a are $S = 1/2$ spin operators at site i . We note that this model has an additional Z_2 symmetry, interchanging spin and orbital degrees of freedom, along the line $x = y$.

Our main conclusion is the groundstate phase diagram of Fig. 1. Phases I, II and III and IV, have been discussed extensively in previous work.¹⁻⁵ In phase I both spin and orbital degrees of freedom are in fully polarized ferromagnetic states. In phase II the orbital degrees of freedom are in the fully polarized ferromagnetic state while the spin degrees of freedom are in the standard antiferromagnetic groundstate and vice versa in phase III. Phase IV is a gapped phase with spontaneous dimerization. Our new results concern phase V. The point on the V-IV phase boundary at $(x, y) = (1/4, 1/4)$ has $SU(4)$ symmetry and is Bethe ansatz integrable.⁶ The $SU(4)$ symmetry follows from the fact that this Hamiltonian is simply a permutation operator, interchanging states on neighboring sites. The low energy theory for this model is known to be the $SU(4)_1$ Wess-Zumino-Witten (WZW) model, with central charge $c=3$, equivalent to 3 decoupled free bosons.¹¹⁻¹³ We show here that the entire extended region V is gapless. (Previous work concluded that only the Z_2 symmetric line $-1/4 < x = y < 1/4$ was gapless.) We show that the renormalization group (RG) flows in region V are to the IV-V phase boundary line. This represents a line of critical points of a rather unusual kind. All critical exponents are unchanged along the line

but there are two different “spin-wave” velocities one for spin and one for orbital degrees of freedom. Their ratio varies continuously along this critical line. They are equal at $(x, y) = (1/4, 1/4)$. At the tri-critical point where II, IV and V merge the orbital velocity goes to 0 while the spin velocity stays finite. Such a vanishing velocity is a natural precursor of a transition into a ferromagnetic phase where the dispersion relation is quadratic, rather than linear, at small wave-vectors.

This behavior can be understood using non-Abelian bosonization techniques.^{7,8} The $SU(4)_1$ WZW model is equivalent to a product of two independent $SU(2)_2$ WZW models, one for spin and one for orbital angular momentum. The $SU(2)_2$ WZW models is itself equivalent to a triplet of Majorana fermions, a representation of the spin-orbital model used by Azaria et al.⁵ However, the low energy components of the spin operators with wave-vectors near $\pm\pi/2$ cannot be represented locally in terms of the Majorana fermions whereas they can be so represented by the WZW models, making this representation more powerful in general. The amplitudes in front of the decoupled spin and orbital terms in the $SU(2)_2 \times SU(2)_2$ WZW Hamiltonian are proportional to the spin and orbital velocities. These are equal for $x=y$ but can be seen to be unequal in general. In order to test the validity of this picture, we predict the finite size spectrum in region V for both periodic and open boundary conditions. This takes the general form:

$$E_i - E_0 = \frac{2\pi}{l} [v_s x_i^s + v_o x_i^o], \quad (1.2)$$

where l is the system length. As usual in conformal field theory (CFT), the finite size gaps are proportional to scaling dimensions of operators corresponding to the states. Under the non-Abelian bosonization, each operator can be written as a product of a spin and orbital operator with the additive scaling dimensions, $x_i^{s,o}$. Of course, at the symmetric point, $v_s = v_o$ and we recover the usual CFT result. As we move around in region V

the velocities change but the scaling dimensions $x_i^{s,o}$ do not. Thus, we may say that this entire region is SU(4) invariant up to a velocity rescaling.

This type of critical behavior is, strictly speaking, not Lorentz invariant and is, in fact, governed by an exactly marginal non-Lorentz invariant operator in the low energy effective Hamiltonian. However, this type of breaking of Lorentz invariance is essentially trivial and is familiar from Tomonaga-Luttinger liquids where the spin and charge velocities are different.

The transition between regions IV and V, along the Z_2 symmetric line, is in a recently discovered generalization of the Kosterlitz-Thouless universality class⁹ characterized by the correlation length (and inverse gap) diverging as:

$$\xi \propto \exp[A(x - x_c)^{-2/3}]. \quad (1.3)$$

We verify our RG conclusions, to some extent, by density matrix renormalization group (DMRG) work for chains of length up to 60. Such numerical verification is rendered very difficult by logarithmic corrections which we also derive.

After this work was essentially completed Ref. (10) appeared on the xxx archive which also discovered the gapless region V. However, there it was concluded from numerical work that region V actually consisted of 3 different gapless phases characterized by the spin and orbital quantum numbers of the lowest excitation. Our Eq. (1.2) predicts crossing of the lowest excited state as the ratio v_s/v_o varies but makes it clear that such a level crossing *does not* correspond to a phase transition. In general different finite size levels cross at different ratios of v_s/v_o ; these crossing points are of no particular significance and region V is just characterized by the line of fixed point with continuously varying velocity ratio.

In the next section we discuss non-abelian bosonization of this model and the RG flows, deducing the phase diagram. In section III we discuss the finite-size spectrum with both periodic and open boundary conditions and in particular, explain the level crossings observed in Ref. (10). We also calculate logarithmic corrections. In Sec. IV we present our DMRG results, corroborating our analytical predictions. Sec. V contains conclusions.

II. NON-ABELIAN BOSONIZATION AND RG ANALYSIS

A convenient way to bosonize this model^{11,12} is to begin with a generalized Hubbard model at a commensurate filling where charge excitations are gapped. Upon bosonizing the fermion model, it is found that the Hubbard interaction only has the effect of gapping the charge bosons leaving various gapless spin-orbital degrees of freedom governed by an effective Hamiltonian which is conformally invariant up to marginal operators. We begin by considering the SU(4) invariant case.

Consider the tight-binding model:

$$H = \sum_j [(-tc_j^{\dagger a\alpha} c_{a\alpha,j+1} + \text{h.c.}) + U(c_j^{\dagger a\alpha} c_{a\alpha,j} - 1)^2], \quad (2.1)$$

where $c_{j\alpha a}$ is an electron annihilation operator, j labels sites and the repeated spin, and orbital indices, represented by Greek and Latin indices respectively, are summed from 1 to 2. We consider the case of 1/4 filling, i.e. 1 particle per site. In the large U limit only states with exactly one particle on every site have low energy, giving the SU(4) invariant version of the spin-orbital model with an exchange interaction of $O(t^2/U)$. The spin and orbital operators are represented by:

$$\vec{S}_i = c_i^{\dagger \alpha a} \frac{\vec{\sigma}_\alpha^\beta}{2} c_{i\beta a}, \quad \vec{T}_i = c_i^{\dagger \alpha a} \frac{\vec{\sigma}_a^b}{2} c_{i\alpha b}. \quad (2.2)$$

The SU(4) symmetric exchange Hamiltonian can be written:

$$H = (1/4) \sum_j S_j^A S_{j+1}^A, \quad (2.3)$$

where

$$S_j^A \equiv c_j^{\dagger \alpha a} (M^A)^{\beta b}_{\alpha a} c_{\beta b,j} \quad (2.4)$$

and the M^A 's are a complete set of 15 4×4 traceless Hermitean matrices normalized so that:

$$\text{tr} M^A M^B = (1/2) \delta^{AB}. \quad (2.5)$$

The factor of 1/4 was inserted in Eq. (2.3) in order that the normalization agree with that of Eq. (1.1) at $x=y=1/4$. A convenient choice of these 15 matrices is:

$$(\sigma^i)_\alpha^\beta \delta_a^b / \sqrt{8}, \delta_\beta^\alpha (\sigma^i)_a^b / \sqrt{8}, (\sigma^i)_\alpha^\beta (\sigma^j)_a^b / \sqrt{8}, \quad (2.6)$$

with $i, j = 1, 2, 3$. Thus the first 6 SU(4) operators are the spin and orbital angular momentum operators and the additional 9 SU(4) operators combine spin and orbital angular momentum. The 15 SU(4) operators, S_j^A are given by the spin and orbital operators \vec{S}, \vec{T} and $S^i T^j$.

We may study the low energy degrees of freedom of this model by keeping only Fourier modes of the fermions near the Fermi points, $\pm\pi/4$. Thus we introduce left and right movers, $\psi, \bar{\psi}$:

$$c_{j\alpha a} \simeq \sqrt{\frac{1}{2}} \left(\psi_{\alpha a}(j) e^{i(\pi/4)j} + \bar{\psi}_{\alpha a}(j) e^{-i(\pi/4)j} \right). \quad (2.7)$$

The hopping term gives, at low energies, a Lorentz invariant free Dirac fermion Hamiltonian density:

$$\mathcal{H} = iv[\psi^\dagger(d/dx)\psi - \bar{\psi}^\dagger(d/dx)\bar{\psi}], \quad (2.8)$$

with effective “velocity of light” given by the Fermi velocity, $v = \sqrt{2}t$.

The Hubbard interaction gives 4 different continuum terms upon dropping all oscillating terms. These can be conveniently written in terms of left and right charge and SU(4) currents:

$$J =: \psi^{\dagger\alpha a} \psi_{\alpha a} ;, \quad J^A = \psi^{\dagger\alpha a} (M^A)_{\alpha\alpha}^{\beta b} \psi_{\beta b} \quad (2.9)$$

where the M^A matrices are discussed in the preceding paragraph. Using the basis of matrices given in Eq. (2.6) we see that the first six SU(4) currents are the spin and orbital currents which we write as J_s^i and J_o^i respectively. We also define right moving currents \bar{J} and \bar{J}^A . The 4 continuum interactions obtained from the lattice Hubbard interaction are:

$$\begin{aligned} \mathcal{H}_{int}/4\pi v = & \lambda_0(J^A J^A + \bar{J}^A \bar{J}^A) + \lambda_1(JJ + \bar{J}\bar{J}) \\ & + g_0 J^A \bar{J}^A + g_c J \bar{J}. \end{aligned} \quad (2.10)$$

The index A is summed over all 15 values and the coupling constants are all proportional to U .

To proceed with an RG analysis of this model it is very convenient to bosonize.^{11–13} In order to keep explicit track of the SU(4) symmetry we use non-abelian bosonization.^{7,8} Various fermion bilinears can be represented in terms of a free charge boson, ϕ_c and an $SU(4)$ matrix field g . The non-interacting action is a sum of the usual free boson action and the WZW action with the integer-valued topological coupling constant having the value $k=1$. Both terms in the bosonized free Hamiltonian are quadratic in currents:

$$\mathcal{H} = (\pi v/4)(JJ + \bar{J}\bar{J}) + (2\pi v/5)(J^A J^A + \bar{J}^A \bar{J}^A). \quad (2.11)$$

It is a remarkable fact¹⁵ that the free fermion Hamiltonian of Eq. (2.8) can also be written in a form quadratic in the currents of Eq. (2.9). This observation is crucial for establishing bosonization. We now consider the effects of the 4 interaction terms in Eq. (2.10). The non-Lorentz invariant interactions, λ_0 and λ_1 renormalize the amplitudes of the free Hamiltonian corresponding to renormalizing the velocities for charge and SU(4) excitations:

$$v_4 \rightarrow v(1 + 5\lambda_0) \quad v_c \rightarrow v(1 + 8\lambda_1). \quad (2.12)$$

The g_c interaction is easily handled since the charge currents are linear in the charge boson:

$$J = (1/\sqrt{8\pi})\partial_- \phi_c \quad \bar{J} = (1/\sqrt{8\pi})\partial_+ \phi_c. \quad (2.13)$$

Thus the charge part of the Lagrangian density (in units where $v_c = 1$) becomes:

$$\mathcal{L}_c \rightarrow (1/2)(1 - g_c/2)(\partial_\mu \phi_c)(\partial_\mu \phi_c). \quad (2.14)$$

g_c can be adsorbed into a rescaling of the charge boson. The g_0 interaction is not so trivial but can be seen to

renormalize to 0 from an initially negative value which it obtains for $U > 0$. Thus, at small U , the low energy theory for the SU(4) Hubbard model is a type of Tomonaga-Luttinger liquid with decoupled gapless charge and SU(4) degrees of freedom. However, as U is increased we expect a phase transition into a phase with gapped charge excitations. This was recently confirmed by $T = 0$ Monte Carlo work.¹⁴ In the continuum description, this transition is driven by an Umklapp term which is of 8th order in the fermion fields:

$$H_{\text{Umklapp}} \propto \psi^{\dagger 12} \psi^{\dagger 21} \psi^{\dagger 22} \psi^{\dagger 11} \bar{\psi}_{11} \bar{\psi}_{12} \bar{\psi}_{21} \bar{\psi}_{22} + h.c. \quad (2.15)$$

Such an interaction is generated at order U^2 . It is irrelevant at small U , being of scaling dimension 4. Under bosonization it can be expressed as a pure charge operator, $\cos 4\sqrt{\pi}\phi_c$. However, as U is increased, the scaling dimension of this operator decreases due to the rescaling of ϕ_c produced by the g_1 interaction. It is expected to become relevant at a critical value of U and produce a gap for charge excitations. Importantly, the effective Hamiltonian for the SU(4) degrees of freedom is expected to remain the gapless SU(4) WZW model with a marginally irrelevant coupling constant g_0 of $O(1)$. The SU(4) velocity parameter cannot be determined exactly by this bosonization approach but its value is known from the Bethe ansatz solution, $v = \pi/8$.

While this method of deriving the $SU(4)_1$ representation of the SU(4) chain is perhaps most familiar to condensed matter physicists it can be also be done more elegantly by simply projecting out the charge degrees of freedom of the free fermions.¹⁷ Either way, the result is that the low energy degrees of freedom of the SU(4) exchange model can be represented as:

$$S_j^A \approx (J^A + \bar{J}^A) + \text{const}[e^{i(\pi/2)j} \text{tr}(gM^A) + h.c.], \quad (2.16)$$

where g is the fundamental unitary 4×4 matrix field of the WZW model. This has scaling dimension $3/4$, so the correlation function decays with power $3/2$. As pointed out by Azaria et al.,⁵ another term, oscillating at $4k_F = \pi$ should also be generated by higher order processes and be included in Eq. (2.16). In the WZW representation, this operator is the dimension 1 primary transforming under the (6,6) representation of $SU(4)_L \times SU(4)_R$. (The 6-dimensional representation of SU(4) is the 2 index antisymmetric tensor representation; i.e. its Young tableau has 1 column and 2 rows.) In our rather cumbersome notation, we may write this tensor as:

$$\Phi_{\{\gamma c, \delta d\}}^{\{\alpha a, \beta b\}}, \quad (2.17)$$

where the indices in curly brackets are antisymmetrized. The additional term in Eq. (2.16) then takes the form:

$$(-1)^j \text{const} \cdot \Phi_{\{\alpha a, \delta d\}}^{\{\alpha a, \beta b\}} (M^A)_{\beta b}^{\delta d}. \quad (2.18)$$

In order to study the effects of $SU(4)$ symmetry breaking, it is convenient to use a different but equivalent non-abelian bosonization of the $SU(4)$ exchange model. We may replace the $SU(4)_1$ WZW model by a sum of 2 decoupled $SU(2)_2$ WZW models representing spin and orbital degrees of freedom. The subscript 2 implies that the topological coupling constant takes the value $k = 2$. One way of arriving at this result is by using a different non-abelian bosonization of the $SU(4)$ Hubbard model in which the fermions are represented by the charge boson plus these 2 WZW models. Alternatively we may use the conformal embedding of this sum of WZW models into the $SU(4)_1$ model. The validity of this representation can be checked from the fermion identity:¹⁶

$$J^A J^A / 5 = (J_s^i J_s^i + J_o^i J_o^i) / 4. \quad (2.19)$$

Thus the Hamiltonian of the non-interacting model is written as a sum of terms quadratic in spin and orbital currents only. The $SU(4)$ matrix field g can be replaced by product of $SU(2)$ matrix fields representing spin and orbital degrees of freedom. These both have scaling dimension $3/8$ in the $SU(2)_2$ WZW model so that their product has the correct dimension $3/4$. Similarly the components of Φ can be expressed as sums of components of the spin-1 primary fields of the $SU(2)_2$ models.

Now consider the effect of breaking the $SU(4)$ symmetry down to $SU(2) \times SU(2)$, corresponding to the general spin-orbital model. We use the field theory approach, adding small anisotropic exchange terms, taking the parameters x, y in the Hamiltonian of Eq. (1.1) to have the values $1/4 + \delta x$ and $1/4 + \delta y$. This leads to the anisotropic corrections to the continuum limit Hamiltonian:

$$\begin{aligned} \delta\mathcal{H}/v = & \frac{4}{\pi} [\delta x (\vec{J}_s \cdot \vec{J}_s + \vec{J}_s \cdot \vec{J}_s) + \delta y (\vec{J}_o \cdot \vec{J}_o + \vec{J}_o \cdot \vec{J}_o)] \\ & + \text{const} [\delta x \vec{J}_s \cdot \vec{J}_s + \delta y \vec{J}_o \cdot \vec{J}_o]. \end{aligned} \quad (2.20)$$

The constant factor is non-universal but we expect it to be positive as can perhaps be seen most simply from the Majorana fermion analysis of Azaria et al.⁵ discussed below.

We first consider the effect of the Lorentz invariant terms. Including the large g_0 term already present at the $SU(4)$ point, the interaction Hamiltonian becomes:

$$\mathcal{H}_{\text{int}} / (4\pi v) = g_0 J^A \bar{J}^A + g_1 \vec{J}_o \cdot \vec{J}_o + g_2 \vec{J}_s \cdot \vec{J}_s. \quad (2.21)$$

Here the bare coupling constant, g_0 has an unknown negative value of $O(1)$ while:

$$g_1 \approx A\delta x, \quad g_2 \approx A\delta y, \quad (2.22)$$

for a positive constant, A .

The corresponding weak coupling β functions can be derived using standard methods. The simplest method is perhaps to just treat these interactions perturbatively in the free fermion theory. This is valid because the gapping of the charge boson by the large Hubbard interaction doesn't effect the renormalization of the coupling

constants in the $SU(4)$ sector or the theory. The result is:

$$\begin{aligned} l \frac{dg_0}{dl} &= 4g_0^2 + 4g_0(g_1 + g_2), \\ l \frac{dg_1}{dl} &= -2g_0g_2 + 2g_1^2, \\ l \frac{dg_2}{dl} &= -2g_0g_1 + 2g_2^2. \end{aligned} \quad (2.23)$$

To understand the solution of these RG equations, it is convenient to first consider the Z_2 symmetric case, $g_1 = g_2$, where they reduce to:

$$\begin{aligned} l \frac{dg_0}{dl} &= 4g_0^2 + 8g_0g_1, \\ l \frac{dg_1}{dl} &= -2g_0g_1 + 2g_1^2 \end{aligned} \quad (2.24)$$

Note that along the Z_2 symmetric line in region V of the phase diagram $g_1 = g_2 < 0$. In this case, the first of Eq. (2.24) implies that g_0 increases (i.e. its magnitude decreases since it is < 0). The second of these equations implies that g_1 initially decreases (increases in magnitude) since initially $|g_0| \gg |g_1|$. This continues until $g_0 = g_1$ after which g_1 begins to increase towards 0 as does g_0 . It is also instructive to notice Eq. (2.24) imply:

$$\frac{1}{2} \frac{d \ln g_0}{d \ln l} = 2(g_0 + 2g_1) = \frac{d \ln(g_0 + g_1)}{d \ln l} + \frac{d \ln g_1}{d \ln l}. \quad (2.25)$$

Thus, along any RG flow:

$$|g_1(g_0 + g_1)|^2 |g_0|^{-1} = \text{constant}, \quad (2.26)$$

This implies, that at long length scales, in region V, $|g_0| \propto g_1^4$. Thus, even though the bare value of $|g_0|$ is much larger than the bare value of $|g_1|$ this situation eventually reverses during the RG flow towards 0 coupling. Some RG trajectories are shown in Fig. 2. Both the non-monotonic flow of g_1 and the fact that, asymptotically $|g_1| \gg |g_0|$ will have important consequences for logarithmic corrections to finite size scaling, discussed in the next sections. We emphasize the remarkable fact that even though the $SU(4)$ symmetry is broken down to $SU(2) \times SU(2)$, this symmetry breaking is irrelevant and the full $SU(4)$ symmetry still appears in the low energy behavior.

On the other hand for the $\delta x \sim g_1 > 0$ case, the RG flow runs away from the critical point $g_0 = g_1 = 0$. This implies that the system has an energy gap and a finite correlation length ξ . We can see the universal behavior of the gap generation by integrating the RG equation (2.24) using Eq.(2.26) to solve for g_0 . Let us consider an initial condition $g_0 = O(1)$ and $g_1 \sim \delta x > 0$. This implies the constant in the right hand side of Eq.(2.26) is proportional to δx^2 . The correlation length ξ corresponds to the scale which makes the running coupling constants diverge

$$\ln \xi = \int_{\delta x}^{\infty} dg_1 \frac{g_1}{2g_1^3 - (C\delta x)^2 - C\delta x \sqrt{2g_1^3 - (C\delta x)^2}} \sim \delta x^{-2/3}, \quad (2.27)$$

where C is a non-universal constant. In this way we obtain the behavior of the correlation function or inverse gap as a function of δx :

$$\Delta \sim \exp[-A(\delta x)^{-\tilde{\nu}}], \quad (2.28)$$

corresponding to a type of generalized Kosterlitz-Thouless behavior discussed extensively in Ref. (9). In this case, $\tilde{\nu} = 2/3$.

Next, we study the Z_2 asymmetric model with $x \neq y$ and hence $g_1 \neq g_2$. Noting that the last 2 equations of Eq. (2.23) are equivalent to:

$$\begin{aligned} l \frac{d(g_1 + g_2)}{dl} &= -2g_0(g_1 + g_2) + 2(g_1^2 + g_2^2), \\ l \frac{d(g_1 - g_2)}{dl} &= 2(g_1 - g_2)[(g_1 + g_2) - g_0], \end{aligned} \quad (2.29)$$

We see that g_0 will still renormalize towards 0 as long as initially $g_1 + g_2 < 0$. In this case, $g_1 + g_2$ initially flows away from 0 but again turns around and flows towards 0 when $g_1^2 + g_2^2 = g_0(g_1 + g_2)$. Similarly, the asymmetry parameter, $g_1 - g_2$ initially increases in magnitude but eventually also flows to 0. It can be seen that for $\delta x + \delta y > 0$, the RG equations predict the development of a finite gap. Thus the phase boundary between regions IV and V should be at a 45° angle to the x-axis, as drawn in Fig. 1.

From considering only Lorentz invariant operators in \mathcal{H}_{int} we would include that Z_2 asymmetry is completely irrelevant in region V since it doesn't alter the flow towards the SU(4) symmetric critical point. However, we must also consider the non-Lorentz invariant interaction terms in Eq. (2.20). It is at this point that it becomes very convenient to use the $SU(2)_2 \times SU(2)_2$ WZW model, which is equivalent to the $SU(4)_1$ model as discussed above. We then see that the non-Lorentz interaction terms just renormalize the coefficients in front of the 2 terms in the non-interaction Hamiltonian:

$$\begin{aligned} \mathcal{H}_0 \rightarrow & \frac{\pi v_o}{2} (\vec{J}_o \cdot \vec{J}_o + \vec{J}_o \cdot \vec{J}_o) \\ & + \frac{\pi v_s}{2} (\vec{J}_s \cdot \vec{J}_s + \vec{J}_s \cdot \vec{J}_s). \end{aligned} \quad (2.30)$$

For small δx and δy , the shift in velocities from the SU(4) value is linear:

$$\begin{aligned} v_o &\approx \pi/8 + B\delta x + C\delta y \\ v_s &\approx \pi/8 + B\delta y + C\delta x. \end{aligned} \quad (2.31)$$

The positive constants B and B are not universal due to renormalization of these non-Lorentz invariant terms in the effective Hamiltonian by the Lorentz invariant terms discussed above. These velocities are, of course,

equal along the Z_2 symmetric line $x = y$. Thus, with Z_2 symmetry, all breaking of SU(4) symmetry is irrelevant. However, also breaking the Z_2 symmetry produces a marginal line of fixed points, which we may regard as the phase boundary between regions IV and V in Fig. 1. Along this line the critical theory is the $SU(2)_2 \times SU(2)_2$ WZW models with unequal v_s and v_o . All critical exponents are constant along this line. The breaking of SU(4) symmetry is thus of a very trivial kind. Nonetheless, it has important consequences for the finite size spectrum, as discussed in the next section. As discussed in the introduction, the transition from phase IV to phase II or III is naturally associated with the vanishing of v_o or v_s respectively.

We remark that the same conclusions can be reached by employing the Majorana fermion representation of the spin-orbital model used by Azaria et al.⁵. The $SU(4)_1$ WZW model is equivalent to 3 free bosons or 6 free Majorana fermions. The two $SU(2)_2$ factors are each equivalent to 3 free Majorana fermions, which transform as vectors under the $SU(2)$ symmetry. Breaking the Z_2 symmetry just gives different velocities to the spin and orbital Majorana fermions. The WZW formulation of the problem is somewhat more natural than the Majorana fermions because all operators in the underlying lattice model can be expressed locally in terms of WZW fields. This is not true in the Majorana fermion representation. The $2k_F$ components of the lattice spin operators are non-local in terms of Majorana fermions. This can be understood by using another equivalence. Each Majorana fermion theory can actually be considered to be an Ising model. This contains order and disorder operators of dimension 1/8 which cannot be expressed locally in terms of the Majorana fermions. The $SU(2)_2$ model is equivalent (locally) to a product of 3 Ising models. In particular, all components of the fundamental SU(2) matrix field of the WZW model, of dimension 3/8 can be expressed as various products of the 3 Ising order and disorder fields. The WZW model is a more natural formulation of this problem than the product of Ising models since it makes the SU(2) symmetries manifest.

We also remark that the spin-orbital model provides a rare example of a lattice model whose critical theory is given by WZW models with central charge $k > 1$. These also occur as critical theories for special integrable SU(2) spin chains of higher spin (with $k = 2s$).²⁰ However, the integrable models represent multi-critical points. Generic spin- s Hamiltonians always renormalize to the $k=1$ WZW model for half-integer s or develop a gap for integer s . The fact that $k > 1$ WZW models represent unstable fixed points can be understood from an RG point of view. They contain relevant operators allowed by symmetry in the context of spin- s Heisenberg models. However, the structure of the spin-orbital model is such as to forbid any relevant operators on the $SU(2)_2 \times SU(2)_2$ fixed line. This extra symmetry can be traced back to the SU(4) invariant model. Translation by 1 site corresponds to multiplying the fundamental SU(4) matrix field by a phase

$e^{i\pi/2}$. Consequently, a produce of 2 of the these fields, which gives the antisymmetric tensor primary field of dimension 1, gets multiplied by a minus sign under translation. Thus both these operators are forbidden from the effective Hamiltonian by translational symmetry. [They are not otherwise forbidden since it is possible to make diagonal $SU(4)$ singlets from both of them.] Using the $SU(2)_2 \times SU(2)_2$ representation, the antisymmetric tensor field of the $SU(4)$ model becomes the two symmetric tensor fields of the two $SU(2)$ models. These must also transform with a minus sign under translation and hence are forbidden, unlike the situation for an $s=1$ Heisenberg model where this operator is allowed in the effective Hamiltonian and produces a gap.

III. FINITE SIZE SPECTRUM

The analysis of the previous section permits a straightforward prediction of the finite size spectrum of this model. This is useful for comparing to numerical simulations in order to test our conjectured phase diagram. The spacing of energy levels vanishes as $1/l$ as the system size l is increased. The coefficients of $1/l$ give scaling dimensions of operators corresponding to the various states. Marginally irrelevant operators give corrections to the finite size spectrum which vanish as $1/l \ln l$. These must be taken into account to obtain reasonable agreement with numerical data for system sizes that are less than exponentially large. We first discuss the finite size spectrum ignoring marginal operators, obtaining only $1/l$ terms. Logarithmic corrections are discussed at the end of this section. We only consider the case where the number of sites is divisible by 4. The generalization to other chain lengths is straightforward but tedious.

We begin by discussing the $SU(4)$ symmetric model. The groundstate energy for a system of length l with periodic boundary conditions (PBC) has the form:

$$E_0 = e_0 l - \pi v c / 6l \quad (3.1)$$

where the central charge, $c = 3$. The finite size energy levels with periodic boundary conditions are given by:

$$E_i - E_0 = (2\pi v / l) x_i, \quad (3.2)$$

where x_i is the RG scaling dimension of the operator corresponding to the excited state i . The lowest excited states for the $SU(4)$ invariant model correspond to the fundamental operator, g of the $SU(4)_1$ WZW model with $x = 3/4$. This transforms under the $(4, \bar{4})$ representation of $SU(4)_L \times SU(4)_R$. This full chiral $SU(4)$ is broken by marginal operators, discussed below. Only the diagonal $SU(4)$ subgroup is an exact symmetry of the lattice model. Under this subgroup the $(4, \bar{4})$ representation decomposes into the adjoint and singlet representations ($16=15+1$). The Hermitean conjugate operator, transforming as $(\bar{4}, 4)$ corresponds to another set of states.

These two sets of states have crystal momenta $\pm\pi/2$ respectively. Thus there are 30 exactly degenerate lowest excited states and two higher singlet states which are degenerate up to log corrections. These states all have crystal momentum $\pm\pi/2$. The next lowest energy excited states transform under the $(6, 6)$ representation of $SU(4)_L \times SU(4)_R$, corresponding to the primary field Φ of dimension $x=1$ discussed in Sec. II. Under diagonal $SU(4)$ $(6,6)$ decomposes as:

$$36 = 1 + 15 + 20. \quad (3.3)$$

Thus we obtain singlet, adjoint and 20 representations all with same energies up to log corrections. The 20 representation is real and has a Young tableau with 2 columns and 2 rows. These states occur at crystal momentum π .

We now consider the effect of breaking the $SU(4)$ symmetries down to $SU(2) \times SU(2)$ spin and orbital symmetries, by giving different velocities to the spin and orbital parts of the energies of these excited states. We represent the quantum numbers of these states by (S, T) the spin and orbital angular momentum of the state. The two sectors both have central charge $c=3/2$, so the groundstate energy is:

$$E_0 = e_0 l - (\pi/6l)(3/2)(v_s + v_o). \quad (3.4)$$

The adjoint representation decomposes into

$$15 \rightarrow (1, 0) + (0, 1) + (1, 1). \quad (3.5)$$

The $x=3/4$ $SU(4)_1$ fundamental field is written as a product of $x=3/8$ fundamental fields of the $SU(2)_2$ WZW models. Thus equal portions of the energies of these states come from the spin and orbital sector. Consequently the energies are all equal for the $(1,0)$, $(0,1)$ and $(1,1)$ states at momenta $\pm\pi/2$:

$$E - E_0 = (2\pi/l)(v_s + v_o)(3/8). \quad (3.6)$$

The same is true for the singlet state with logarithmically higher energy. On the other hand, the 6 representation of $SU(4)$ decomposes into $(1,0)+(0,1)$. Thus the various components of the $(6, 6)$ primary field become:

$$[(S_L, T_L), (S_R, T_R)] = [(1, 0), (1, 0)], \quad [(0, 1), (0, 1)], \\ [(0, 1), (1, 0)] \text{ and } [(1, 0), (0, 1)] \quad (3.7)$$

primary fields in the $SU(2)_2 \times SU(2)_2$ representation. The spin 1 primary field of the $SU(2)_2$ WZW model has $x=1$ (left and right scaling dimensions $1/2$). Thus we see that for the 4 different sets of states listed in Eq. (3.7), the spin and orbital dimensions are:

$$(x_s, x_o) = (1, 0), \quad (0, 1), \quad (1/2, 1/2), \quad (1/2, 1/2) \quad (3.8)$$

respectively. The energies of the various states are given by Eq. (1.2). Finally we may decompose these states with respect to the exact diagonal $SU(2) \times SU(2)$ symmetry. Note in particular that there are states with quantum numbers $(S, T) = (2, 0)$ and $(0, 2)$ with energies

$$E_i - E_0 = 2\pi v_s/l, \text{ and } 2\pi v_o/l \quad (3.9)$$

respectively.

Close to the Z_2 symmetric case, $v_s \approx v_o$, the lowest states all have energy $(2\pi/l)(3/8)(v_s + v_o)$ up to log corrections. These states include the $(S, T) = (1, 1)$ state which is in fact lowest due to log corrections. On the other hand, as the ratio v_s/v_o is decreased a level crossing eventually occurs and the lowest states have energy $(2\pi v_s/l)$. These states include the $(S, T) = (2, 0)$ state which is in fact lowest due to log corrections. This occurs when

$$(3/8)(v_s + v_o) = v_s, \quad (3.10)$$

i.e. $v_s = (3/5)v_o$. Thus we expect the quantum numbers of the lowest energy state with periodic boundary conditions to change from $(S, T) = (1, 1)$ to $(2, 0)$ as we move away from the Z_2 symmetric line, $x = y$. Note that this level crossing will occur along a line in the (x, y) plane which is a finite distance away from the Z_2 symmetric line $x = y$. Exactly such behavior was observed in the finite size spectrum with PBC in Ref. (10). However, the present theory makes it clear that this is certainly not a phase transition line. All critical exponents have the same value on both sides of this line. The same set of low energy states occur on both sides. The energies are merely shifted by the ratio v_s/v_o .

We now consider the case of open boundary conditions (OBC). Much longer chains can be studied with OBC using DMRG and our results presented in the next section are all for OBC. In this case the groundstate energy is given by:

$$E_o = e_0 l + e_1 - (\pi/24l)(3/2)(v_s + v_o). \quad (3.11)$$

A non-universal boundary energy, e_1 , appears and the $1/l$ term is reduced by a factor of 4. The energy gaps are given by:

$$E_i - E_0 = (\pi/l)(v_s x_s^i + v_o x_o^i). \quad (3.12)$$

The prefactor is smaller by 2 than in Eq. (1.2) for the PBC case. More importantly, the dimensions, x are different in this case, corresponding to chiral conformal towers taken from the left moving sector only. For the $SU(4)_1$ WZW model only the conformal tower of the identity operator occurs for OBC. Thus the lowest excited states transform under the adjoint representation of $SU(4)$ and correspond to the 15 chiral current operators J^A . As discussed in the previous section these decompose into pure spin or orbital operators and mixed operators. The mixed operators have $(S, T) = (1, 1)$ and $(x_s, x_o) = (1/2, 1/2)$ corresponding to a product of the (chiral) spin 1 primary operators of the $SU(2)_2$ WZW models. Thus we obtain the energies:

$$\begin{aligned} E_{(1,0)} - E_{(0,0)} &= \pi v_s/l \\ E_{(0,1)} - E_{(0,0)} &= \pi v_o/l \\ E_{(1,1)} - E_{(0,0)} &= (\pi/2l)(v_s + v_o), \end{aligned} \quad (3.13)$$

where $E_{(0,0)}$ refers to the groundstate energy. The next excited states have $x = 2$ but we do not consider them here. One of the above states will always have lowest energy. A level crossing occurs at the Z_2 symmetric line, $v_s = v_o$. Note that:

$$E_{(1,1)} = [E_{(1,0)} + E_{(0,1)}]/2 \quad (3.14)$$

ignoring log corrections. We will test this relation numerically in the next section.

Finally we consider log corrections, coming from marginal operators. Note that these take quite a different form at the $SU(4)$ invariant point, $(x, y) = (1/4, 1/4)$ than anywhere else in region V. This is because the only marginally irrelevant coupling constant is g_0 defined in Eq. (2.10) in the $SU(4)$ symmetric case. On the other hand, when the $SU(4)$ symmetry is broken, even in the case where the Z_2 symmetry is preserved, g_0 flows to zero much faster than $g_1 \approx g_2$ defined in Eq. (2.21) according to our analysis of the β functions in the previous section, as illustrated in Fig. 2. Thus, in this case, we may asymptotically ignore g_0 and consider only $g_1 = g_2$ which gives different log corrections than does g_0 . At intermediate lengths we may expect very complicated finite size corrections corresponding to the RG flows discussed in the previous section. In particular, we might expect log corrections due to g_0 out to some crossover length and then log corrections due to $g_1 = g_2$ for longer lengths. Furthermore, the fact that $|g_1|$ and $|g_2|$ may initially *increase* before eventually decreasing, as illustrated in Fig. 2, means that the amount of breaking of $SU(4)$ symmetry may at first appear to *increase* with increasing length before eventually starting to decrease. Evidence for such behavior is presented in the next section.

Log corrections away from the $SU(4)$ point, at long distances, follow immediately from earlier work on the ordinary $s=1/2$ Heisenberg model since the marginal operator, $\vec{J}_s \cdot \vec{J}_s$, is the same one that occurs in that case.^{18,19} (Leading log corrections are independent of the Kac-Moody central charge, k .) We must merely add the corrections twice in the spin and orbital sector, with the corresponding velocities inserted.

We first consider PBC. The log corrections to the energy gaps for any Virasoro primary states with left and right spin \vec{S}_L and \vec{S}_R and left and right orbital angular momentum \vec{T}_L and \vec{T}_R are:

$$\delta E = -\frac{2\pi}{l \ln l} [v_s \vec{S}_L \cdot \vec{S}_R + v_o \vec{T}_L \cdot \vec{T}_R]. \quad (3.15)$$

In particular, some of the lowest energies, including log corrections, are given by:

$$\begin{aligned} E_{(1,1)} - E_{(0,0)} &= \frac{2\pi}{l} (v_s + v_o) \left(\frac{3}{8} - \frac{1}{4 \ln l} \right) \\ E_{(1,0)} - E_{(0,0)} &= \frac{2\pi}{l} \left[v_s \left(\frac{3}{8} - \frac{1}{4 \ln l} \right) + v_o \left(\frac{3}{8} + \frac{3}{4 \ln l} \right) \right] \\ E_{(2,0)} - E_{(0,0)} &= \frac{2\pi}{l} v_s \left(1 - \frac{1}{\ln l} \right). \end{aligned} \quad (3.16)$$

Note in particular that, for $v_s = v_o$, the lowest excited state has quantum numbers (1,1). We also see that the value of v_s/v_o at which the (2,0) state becomes the lowest excited state depends somewhat on l , approaching 3/5 at large l .

We now turn to OBC. In this case, states are classified by only a single spin and orbital quantum number: S and T. The general log corrections for excited states are given by:

$$\delta E = -\frac{\pi}{2l \ln l} [v_s S(S+1) + v_o T(T+1)]. \quad (3.17)$$

The energies of the lowest excited states, including log corrections are given by:

$$\begin{aligned} E_{(1,1)} - E_{(0,0)} &= \frac{\pi}{l} (v_s + v_o) \left(\frac{1}{2} - \frac{1}{\ln l} \right) \\ E_{(1,0)} - E_{(0,0)} &= \frac{\pi}{l} v_s \left(1 - \frac{1}{\ln l} \right) \\ E_{(0,1)} - E_{(0,0)} &= \frac{\pi}{l} v_o \left(1 - \frac{1}{\ln l} \right). \end{aligned} \quad (3.18)$$

Note that for $v_s = v_o$, (1,1) is the lowest excited state.

Finally we give log corrections at the SU(4) point, $(x, y) = (1/4, 1/4)$. For PBC the general formula can be written:

$$\delta E = -\frac{\pi v}{l \ln l} S_L^A S_R^A, \quad (3.19)$$

a straightforward generalization of the SU(2) case. We may write:

$$\begin{aligned} S_L^A S_R^A &= (1/2)[(S_L^A + S_R^A)(S_L^A + S_R^A) - S_L^A S_L^A - S_R^A S_R^A] \\ &= (1/2)[C - C_L - C_R], \end{aligned} \quad (3.20)$$

where C , C_L and C_R are the quadratic Casimir invariants for the diagonal SU(4) group and for $SU(4)_L$ and $SU(4)_R$ groups.

For OBC the corresponding formula is:

$$\delta E = -\frac{\pi v}{4l \ln l} S^A S^A = -\frac{\pi v}{4l \ln l} C. \quad (3.21)$$

The quadratic Casimir is $C = 4$ for the adjoint representation. Thus the lowest excited states have energy:

$$E - E_0 = \frac{\pi v}{l} \left(1 - \frac{1}{\ln l} \right). \quad (3.22)$$

The velocity, in this case, is determined from the Bethe ansatz solution to have the value, $v = \pi/8$.

We emphasize that these formulas only apply for the exactly SU(4) invariant model. For any other points in region V we must use the formulas of the previous paragraphs. Despite the fact that SU(4) symmetry breaking is irrelevant (up to a velocity rescaling) it acts, in a sense, like a relevant perturbation as far as log corrections are concerned. This simply reflects the fact that the RG flow approaches the SU(4) invariant fixed point along a different universal trajectory when SU(4) is broken than when it is unbroken.

IV. DENSITY MATRIX RENORMALIZATION GROUP RESULTS

We now discuss our DMRG calculations.²¹ We keep $m = 1100$ states in DMRG calculation and the biggest truncation error is 5×10^{-6} . We calculate for chains with open boundary conditions with length up to $l = 60$.

Our DMRG calculation is a continuation of previous studies on this model.^{10,3} We will use the ground state energies, which are most accurately calculated by DMRG²², to sketch the phase diagram. As pointed out in Sec. II, the phase transition between phase IV and V is of infinite order.⁵ Thus the singularity of the ground state energy $e(x, y)$ as function of parameter (x, y) in Hamiltonian (1.1) is not obvious. The second derivative of $e(x, y)$ goes to zero roughly exponentially when we move close to the transition point $x = y = 1/4$ from the dimerized phase along the $x = y$ line. We use this property of the infinite order phase transition to sketch the boundary between the gapless phase and the dimerized phase. The phase boundaries into the ferromagnetic phases II and III are determined by a level crossing. The final phase diagram is drawn in Fig. 1.

We now discuss other aspects of our results for region V. At the SU(4) symmetric point, $(x, y) = (1/4, 1/4)$, the lowest excited states are a degenerate set with quantum numbers (S,T)=(1,1), (1,0) and (0,1). This energy gap is compared to the prediction of Eq. (3.22) in Fig. 3, showing good agreement.

When we move away from the SU(4) point into region V along the $x = y$ line of the phase diagram, the energy of the (1,0) excitation will have a finite gap above the energy for of the (1,1) excitation. Let's call this energy difference ΔE . We will measure ΔE by the smallest energy excitation in the system. We use the energy of the (1,1) excitation as the energy unit for ΔE . ΔE represents roughly the distance of the system from the SU(4) invariant model and so is like $g_1 = g_2$ in Fig. 2. When $\Delta E = 0$, our system is SU(4) invariant and $g_1 = g_2 = 0$. When we move farther away from the SU(4) point along the $x = y$ line in the SU(4) gapless phase, ΔE increase and so does $g_1 = g_2$. In the RG flow diagram Fig. 2, we see that when bare $g_1 = g_2$ is small for short chain, $g_1 = g_2$ will first flow away from g_0 axis. So we will also observe ΔE increase when chain length is small for (x, y) close to the SU(4) point (1/4, 1/4). We demonstrate these RG properties in Fig. 4.

It is difficult to obtain data for long chains to demonstrate the logarithmic scalings show in Eq.(3.18). Due to the complex RG flow as we show in Fig. 2 and Fig. 4, very long chains are needed to study this large l scaling. For the Z_2 symmetric $SU(2) \times SU(2)$ model (where $x = y$), we have demonstrated the RG flow numerically in previous paragraph.

For the non- Z_2 symmetric case, it is even more difficult to verify phase V numerically. We show some evidence to support that there is a gapless phase in the central part

V of the phase diagram in Fig. 1 by fitting simple $1/l$ and $1/\log l$ scaling. For an arbitrary point in the $SU(4)$ gapless phase $x = 1/4$ and $y = 1/8$, we plot $(E_{(i,j)} - E_{(0,0)})/\sin(\frac{\pi}{l+1})$ vs. $1/\ln l$ in Fig. 5. The fitting line in the figure shows that $(E_{(i,j)} - E_{(0,0)}) \rightarrow \frac{\pi}{4}$ for our calculation indicating that the phase V is gapless. We point out that there is no singularity in the ground state energy $e(x, y)$ at the symmetric line $x = y$ in the $SU(4)$ phase either. In the extended gapless phase V, there are two spin velocities v_s and v_o as discussed in the previous sections. In Fig. 5, we have drawn

$$\begin{aligned} v_s(l) &\equiv (E_{(1,0)} - E_{(0,0)})/\sin(\frac{\pi}{l+1}), \\ v_o(l) &\equiv (E_{(0,1)} - E_{(0,0)})/\sin(\frac{\pi}{l+1}), \\ v_{(1,1)}(l) &\equiv (E_{(1,1)} - E_{(0,0)})/\sin(\frac{\pi}{l+1}). \end{aligned} \quad (4.1)$$

We have also drawn

$$\frac{v_s + v_o}{8v_{11}} = \frac{(E_{10} - E_{00}) + (E_{01} - E_{00})}{8(E_{11} - E_{00})} \quad (4.2)$$

in Fig. 5. We see that the predicted relation $E_{11} = (E_{10} + E_{01})/2$ which, from Eq. (3.18), should be true up to log corrections, holds quite accurately for all l shown. The numerical results show that the difference between E_{11} and $(E_{10} + E_{01})/2$ is less than five percent in our short chain calculation.

In summary, we studied the $SU(2) \times SU(2)$ spin-orbital model. By a renormalization group study around the $SU(4)$ point we showed there is an extended gapless phase both in the Z_2 symmetric model $x = y$ and the asymmetric model $x \neq y$. This phase has $SU(4)$ symmetry at low energies after rescaling the different spin and orbital velocities. The critical theory may also be viewed as a product of $SU(2)_2$ WZW models for spin and orbital degrees of freedom. We studied the phase transitions from the gapless antiferromagnetic phase with $SU(4)$ symmetry to the dimer phase and to the ferromagnetic phases.

We used the ground state energy calculated by DMRG to sketch out the phase diagram. DMRG calculation also shows evidence for an extended gapless phase by giving a leading $1/l$ finite size scaling of the gap for chain length up to 60 and verifying other aspects of the RG predictions.

NOTE ADDED: After posting this preprint another preprint by Azaria et al.²³ appeared that has much overlap with this one. It analyses the complicated scaling of the gap in region IV near the IV-V phase boundary in the general case, without assuming Z_2 symmetry. An incorrect statement that we made about this in the first version of our preprint has been removed. [23] also studies the shape of the IV-V phase boundary near the $SU(4)$ point analytically, showing that it has the opposite curvature to what is drawn in our Fig. 1. It is possible that the phase boundary has zero curvature points close

to the $SU(4)$ point so that the phase boundary drawn in Fig. 1 is roughly correct. On the other hand, there are non-zero marginal coupling constants present along the phase boundary so that it is difficult to determine its accuracy from finite size data and it is possible that the boundary drawn in Fig. 1 is quite inaccurate.

IA would like to thank Rajiv Singh for helpful discussions. This research was supported in part by NSERC of Canada and by the N.S.F. under Grant. No. PHY94-07194.

-
- ¹ D.P. Arovas and A. Auerbach, Phys. Rev. B **52**, 10114 (1995).
 - ² Y. Q. Li, M. Ma, D. N. Shi, and F. C. Zhang, Phys. Rev. Lett. **81** 3527 (1998).
 - ³ S. K. Pati and R. R. P. Singh, Phys. Rev. Lett. **81**, 5406 (1998)
 - ⁴ A. K. Kolezhuk and H. J. Mikeska, Phys. Rev. Lett. **80** 2709 (1998)
 - ⁵ P. Azaria, A.O. Gogolin, P. Lecheminant, and A.A. Nersisyan, preprint cond-mat/9903047
 - ⁶ G. V. Uimin, JETP Lett. **12**, 225 (1970);
C. K. Lai, J. Math. Phys. **15**, 1675 (1974);
B. Sutherland, Phys. Rev. B **12**, 3795 (1975).
 - ⁷ E. Witten, Comm. Math. Phys. **92**, 455 (1984).
 - ⁸ V. Knizhnik and A. Zamolodchikov, Nucl. Phys. **B247**, 83 (1984).
 - ⁹ C. Itoi and H. Mukaida, cond-mat/9711308 to appear in Phys. Rev. E.
 - ¹⁰ Y. Yamashita, N. Shibata, and K. Ueda, cond-mat/9908237.
 - ¹¹ I. Affleck, Nucl. Phys. **B265**,409 (1986) .
 - ¹² I. Affleck, Nucl. Phys. **B305**, 582 (1988).
 - ¹³ S. V. Prokovskii and A. M. Tsvelik, Sov. Phys. JETP **66**,1275 (1987)
 - ¹⁴ R. Assaraf, P. Azaria, M.Caffarel and P. Lecheminant, Phys. Rev. **B60**, 2299 (1999).
 - ¹⁵ See Ref, (11), Eq. (2.29).
 - ¹⁶ See Ref, (11), Eq. (2.74).
 - ¹⁷ C. Itoi and M. -H. Kato, Phys. Rev. B **55**, 8295 (1997).
 - ¹⁸ I. Affleck, D. Gepner, H.J. Schulz and T. Ziman, J. Phys. **A22**, 511 (1989).
 - ¹⁹ I. Affleck and S. Qin, cond-mat/9907284, J. Phys. **A**, to appear.
 - ²⁰ I. Affleck and F.D.M. Haldane, Phys. Rev. **B36**, 5291 (1987).
 - ²¹ S.R. White, Phys. Rev. Lett. **69**, 2863 (1992); Phys. Rev. B **48**, 10345 (1993).
 - ²² S.R. White and D.A. Huse, Phys. Rev. B **48** 3844 (1993).
 - ²³ P. Azaria, E. Boulat and P. Lecheminant, preprint, cond-mat/9910218.

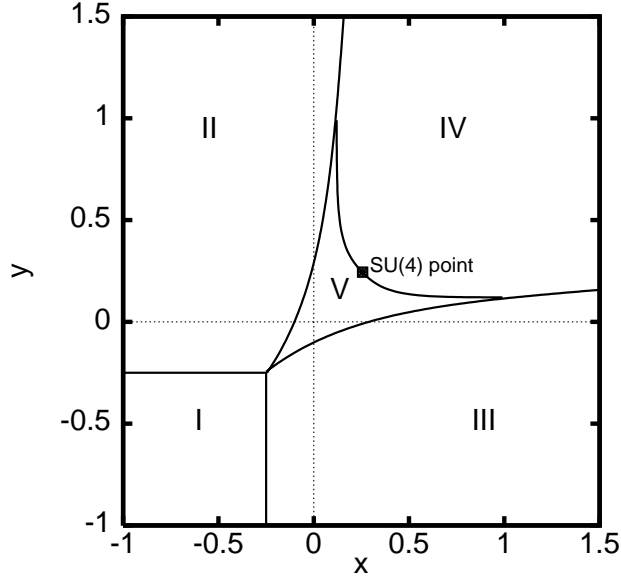


FIG. 1. Phase diagram for model Hamiltonian (1.1). In Phase I, ground state is composed of fully polarized Ferromagnetic (FM) states for both spin S and orbital T . In phase II (phase III), the ground states are antiferromagnetic (AF) for S and FM for T (AF for T and FM for S). Phase IV is a dimerized phase.³ Phase V is a gapless phase.

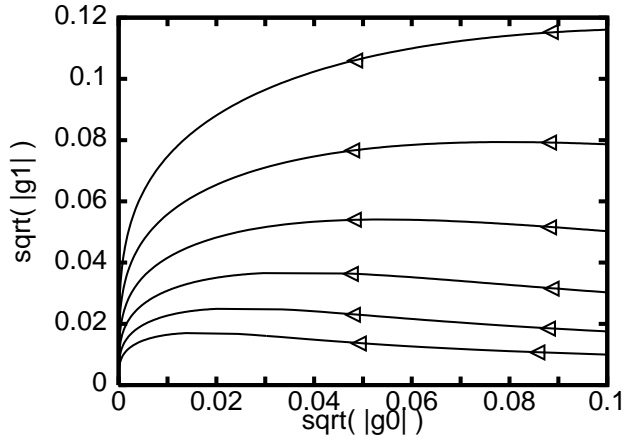


FIG. 2. Renormalization flow for $g_0 < 0$ and $g_1 = g_2 < 0$ according to Eq.(2.26). They flow to zero, the level 1 $SU(4)$ WZW model. We use square root for $|g_0|$ and $|g_1|$ to show the small coupling region clearly.

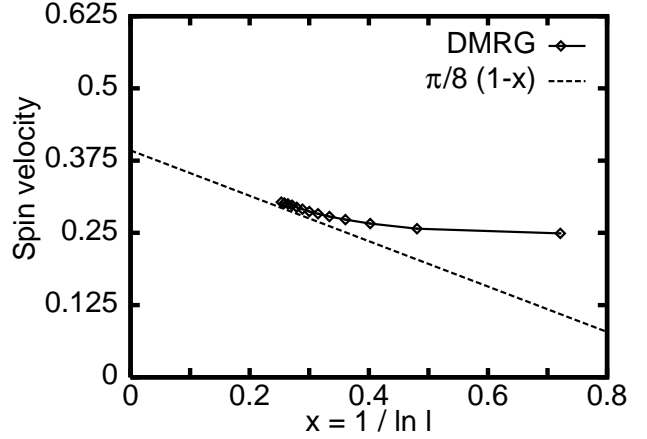


FIG. 3. The scaling of the excitation energy for $SU(4)$ point. The difference between the ground state energy and first excited state energy is plotted as $v_s = (E_{(1,1)} - E_{(0,0)}) / \sin(\frac{\pi}{l+1})$ vs. $1/\ln l$. The fitting line is $(\pi/8)(1 - 1/\ln l)$.

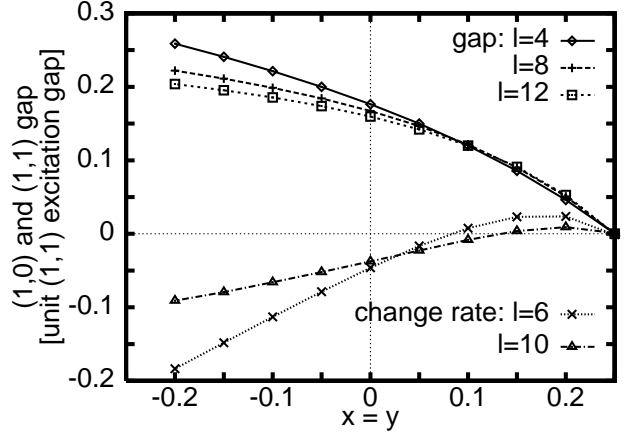


FIG. 4. Energy gap ΔE and its rate of change $d\Delta E(l)/dl$ between triplet-singlet excitation and triplet-triplet excitation on $x = y$ line in $SU(4)$ gapless phase. When $x = y$ is much smaller than the $SU(4)$ point magnitude $x = y = 1/4$, the energy gap ΔE is bigger. But the rate of change for short chain is positive for small deviation from $x = y = 1/4$ and negative for big deviation from $x = y = 1/4$. This is in agreement with the RG flow in Fig. 2.

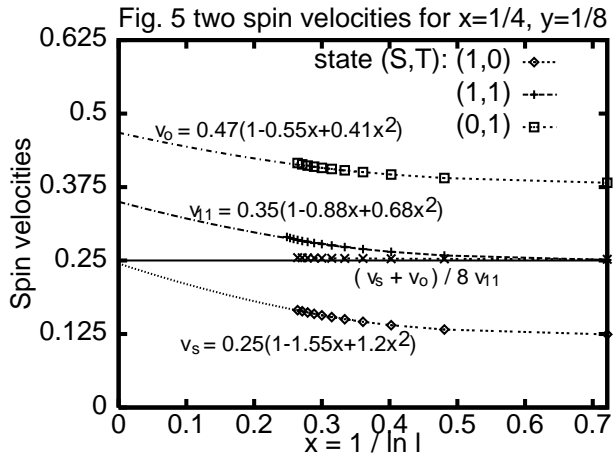


FIG. 5. The scaling of the excitation energies at $(x, y) = (1/4, 1/8)$ in phase V of Fig. 1. The difference between the ground state energy $E_{(0,0)}$, and the excited state energies $E_{(i,j)}$, ($S = i, T = j$) are plotted as $v_{ij} \equiv (E_{(i,j)} - E_{(0,0)}) / \sin(\frac{\pi}{l+1})$ vs. $1/\ln l$. $(v_s + v_o)/8v_{11}$ is plotted and reference line at magnitude 0.25 has been drawn. Fitting lines shows that $v_s \sim 0.26$, $v_o \sim 0.47$, and $v_{11} = (v_s + v_o)/2 \sim 0.35$ in large l limit.